

## PVT<sub>x</sub> Measurements of the Carbon Dioxide + 2,3,3,3-Tetrafluoroprop-1-ene Binary System

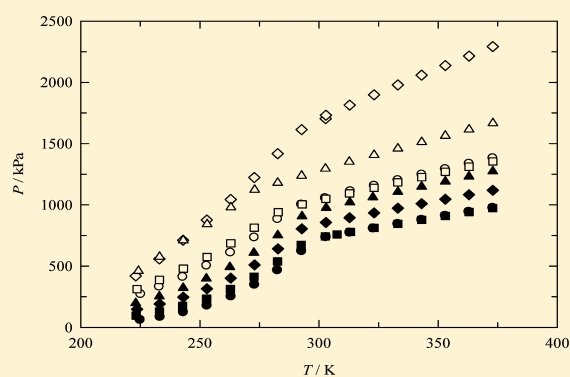
Paper presented at the Nineteenth European Conference on Thermophysical Properties, August 28 to September 1, 2011, Thessaloniki, Greece.

G. Di Nicola,<sup>\*,†</sup> C. Di Nicola,<sup>†</sup> A. Arteconi,<sup>†</sup> and R. Stryjek<sup>‡</sup>

<sup>†</sup>Dipartimento di Energetica, Università Politecnica delle Marche, Via Brecce Bianche 60100, Ancona, Italy

<sup>‡</sup>Institute of Physical Chemistry, Polish Academy of Sciences, 01-224 Warsaw, Poland

**ABSTRACT:** In this work, the PVT<sub>x</sub> properties of carbon dioxide + 2,3,3,3-tetrafluoroprop-1-ene were measured by an isochoric apparatus. The experiment covered both two-phase and superheated vapor regions and have been performed a total of eight isochores within a temperature range that spanned from (223 to 373) K and within a pressure range from (62 to 2292) kPa. Our experimental results were correlated with the Carnahan–Starling–DeSantis equation of state (CSD EoS) and predicted with REFPROP 9.0. Coefficients for the CSD EoS were derived from the experimental data. Results in the two-phase region showed a good agreement with the CSD equation and a strong disagreement with the REFPROP 9.0. Data in the superheated vapor region were also predicted by extrapolating coefficients for the CSD EoS at higher temperatures. The agreement with CSD EoS for the superheated vapor region experimental data was also good. The vapor–liquid equilibrium (VLE) behavior of the studied binary system from the experimental data was also derived.



### INTRODUCTION

For a lower impact on the environment, the European Union decided to ban refrigerants with a global warming potential (GWP) over 150 in automobile air conditioning. This has resulted in a search to find alternatives to a commonly used fluid, R134a (GWP = 1430 for a 100 year time horizon).

R1234yf is a hydrofluoroolefin, a new refrigerant, recently proposed by the chemical industry. It is a non-ozone-depleting substance, having an atmospheric lifetime of 11 days. Its GWP is approximately 12 for a 20 year time horizon and 4 for a 100 year time horizon. Its thermophysical properties have been studied by our laboratory in previous papers.<sup>1,2</sup> One of the main drawbacks of R1234yf is its mildly flammability, having a small gap between lower and upper flammability limits.

Among natural refrigerants, we focused our interest on carbon dioxide,<sup>3,4</sup> particularly because it is nonflammable and it has a low toxicity. Although carbon dioxide has a GWP = 1 and an ozone depletion potential (ODP) that is zero, it has some restrictions due to its thermophysical properties. Additionally, technical issues regarding the use of carbon dioxide remain unresolved by the industry, and the very high system pressures require a total redesign of several system components.

To overcome the drawbacks of both carbon dioxide and R1234yf considered as pure fluids and searching for new perspective refrigerant mixtures for low temperature industrial applications, we focused our attention on a binary system containing both carbon dioxide and R1234yf.

In this paper, the PVT<sub>x</sub> properties of the carbon dioxide + R1234yf were measured by an isochoric apparatus over a wide temperature and pressure range.

### EXPERIMENTAL SECTION

**Chemicals.** Data for each chemical sample are reported in Table 1. Carbon dioxide was supplied by Sol SpA. The sample

**Table 1. Information for Each Chemical Sample**

chemical name	source	initial mole fraction purity	purification method	final mole fraction purity	analysis method
carbon dioxide	Sol SpA	0.9999			
R1234yf <sup>a</sup>	Archema	0.9987	freezing, evacuating, and thawing	0.9995	GC <sup>b</sup>

<sup>a</sup>2,3,3,3-Tetrafluoroprop-1-ene. <sup>b</sup>Gas chromatography.

of R1234yf was produced by the French group Arkema and donated by Centro Ricerche FIAT, Italy. It was then degassed to remove air and other noncondensable gases by immersing it in liquid nitrogen and evacuating. The sample was then brought

**Received:** September 29, 2011

**Accepted:** January 3, 2012

**Published:** January 18, 2012

to room temperature and was again subjected to the freezing, evacuating, and thawing process. This procedure was repeated several times. The purity of carbon dioxide and R1234yf was checked by gas chromatography using a thermal conductivity detector and was found to be better than 99.99 % and 99.95 % on a molar basis, respectively, basing all estimations on an area response.

**Apparatus.** The experimental setup is illustrated in Figure 1. The main modification to the original apparatus concerned the twin

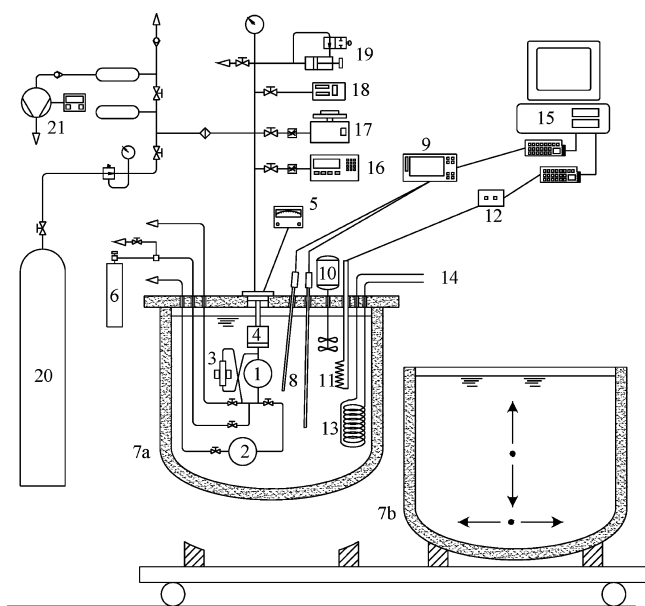


Figure 1. Schematic view of the experimental setup.

thermostatic baths (7) filled with different silicone oils (Baysilone M10 and Baysilone M100, Bayer). After charging with the sample mixture, the setup can be operated over two temperature ranges, from (210 to 290) K and from (290 to 360) K, depending on which bath is used. The thermostatic baths are easy to move due to the new configuration of the system. The spherical cells and pressure transducer are immersed in one of the two thermostatic baths (7). An auxiliary thermostat (14) is used to reach the below-ambient temperatures. The pressure and temperature data acquisition systems remained the same as in the previous apparatus<sup>5</sup> and will be only briefly described here.

An AISI 304 stainless steel spherical cell (1) containing the refrigerant sample is connected to a differential diaphragm pressure transducer (4) coupled to an electronic null indicator (5). In the new setup the transducer and sphere were placed vertically, and a magnetic pump (3) for mixing the sample was connected to the sphere. A second spherical cell (2) was also connected and used for volume calibration. Because of the complex volume of the isochoric cell (1), its total volume (including the piping, the pressure transducer cavity, and the magnetic pump volumes) was calibrated according to the classic Burnett calibration procedure, adopting helium as the reference fluid. After estimating the apparatus constant  $N = (V_1 + V_2)/V_1$ , the auxiliary cell volume,  $V_2$ , was measured by filling it with distilled water. Finally, the volume of the measurement cell,  $V_1$ , was found to be  $273.5 \pm 0.3 \text{ cm}^3$  at room temperature, based on several expansions from cell (1) to cell (2).

A PID device was used to control the temperature, which was measured using a calibrated resistance thermometer; the total

uncertainty of the temperature measurements was  $\pm 0.02 \text{ K}$ . The uncertainty in the pressure measurements stems from the uncertainty of the transducer and null indicator system and the pressure gauges. The uncertainty of the digital pressure indicator (Ruska, model 7000) is  $\pm 0.003 \%$  of its full scale (6000 kPa). Temperature fluctuations due to bath instability can also affect the total uncertainty in the pressure measurement, which was nonetheless found to be less than  $\pm 1 \text{ kPa}$ .

**Experimental Procedure.** Mixtures were prepared using the gravimetric method. First of all, the pure samples were charged in different bottles, degassed to remove noncondensable gases and air, and then weighed with an analytical balance (uncertainty  $\pm 0.3 \text{ mg}$ ). After evacuating the cell, the bottles were then emptied into the cell immersed in the bath. The mixtures were charged in the vapor phase. The bottles were weighed again, and the mass of the charge was calculated from the difference between the two masses. The dispersion of the mass inside the duct was estimated to be between (0.01 and 0.06) g, depending on the charging temperature, pressure, and molar mass of the fluid, and finally subtracted from the total mass of the sample. The uncertainty in the mass was estimated to be lower than  $\pm 0.9 \text{ mg}$ .

The uncertainty for the mass yields an uncertainty for the molar fraction that can be estimated to be constantly lower than 0.001 in mole fraction. Taking into account the uncertainty in the charged mass and in the isochoric cell volume, we estimated the uncertainty in molar volume to be always lower than  $\pm 5 \cdot 10^{-3} \text{ dm}^3 \cdot \text{mol}^{-1}$ . In addition, it is worth it to mention that all changes of molar volumes along temperature depend only on changes in the isochoric cell volumes, also considering the correction for thermal expansion and pressure distortion, as reported elsewhere.<sup>6</sup>

After reaching the experimental temperature, the mixing pump was activated for about 15 min, and, next, the mixture was allowed to stabilize for about 20 min before the data recording. After having charged each mixture composition, the temperature was increased step by step.

## RESULTS AND DISCUSSION

The temperature and pressure ranges are shown in Table 2, along with the mixture's composition and the number of moles charged. The  $P,T$  isochoric sequence is also shown in Figure 2.

Table 2. Measurements at Bulk Compositions  $z_1$  and Masses  $m_1$  and  $m_2$  for the  $\text{CO}_2$  (1) + R1234yf (2) System over the Temperature Range  $\Delta T$  and Pressure Range  $\Delta P$

series	$z_1$	$\Delta T$	$\Delta P$	$n$	$m_1$	$m_2$
		K	kPa			
1	0.051	225–373	62–976	0.0954	0.215	10.322
2	0.160	223–373	96–973	0.0940	0.660	9.005
3	0.266	224–373	148–1119	0.1075	1.256	8.999
4	0.365	223–373	198–1273	0.1225	1.968	8.872
5	0.480	225–373	271–1381	0.1323	2.796	7.838
6	0.574	224–373	312–1354	0.1282	3.236	6.232
7	0.662	223–373	420–2292	0.2250	6.559	8.664
8	0.754	224–373	460–1667	0.1580	5.245	4.433

On the basis of the analysis of the slope of each  $T,P$  sequence, the experimental points were each attributed either to the superheated or to the two-phase region. Table 3 shows the experimental data within the vapor–liquid equilibrium (VLE) boundary, while Table 4 contains the  $PVTx$  data.

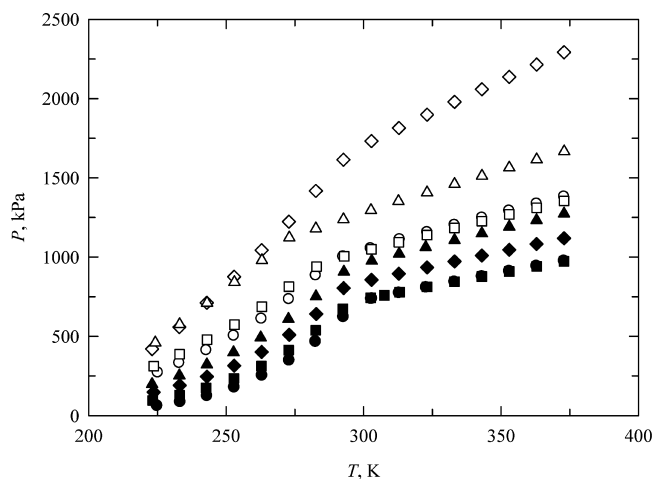


Figure 2. Experimental  $P$ – $T$  data: ●,  $z_1 = 0.051$ ; ■,  $z_1 = 0.160$ ; ◆,  $z_1 = 0.266$ ; ▲,  $z_1 = 0.365$ ; ○,  $z_1 = 0.480$ ; □,  $z_1 = 0.574$ ; ◇,  $z_1 = 0.662$ ; △,  $z_1 = 0.754$ .

Table 3. Experimental Molar Volumes  $V$  as a Function of Pressure  $P$  and Temperature  $T$  at Charged Composition  $z_1$  in the Two-Phase Region for the  $\text{CO}_2$  (1) + R1234yf (2) System

$T$ K	$P$ kPa	$V$ $\text{dm}^3\cdot\text{mol}^{-1}$	$T$ K	$P$ kPa	$V$ $\text{dm}^3\cdot\text{mol}^{-1}$
$z_1 = 0.051$					
224.91	61.7	2.894	272.66	609.0	2.258
233.25	86.7	2.895	282.69	751.6	2.259
243.07	124.7	2.896	$z_1 = 0.480$		
252.97	179.0	2.897	225.14	271.4	2.063
263.06	253.3	2.899	232.92	331.8	2.063
272.93	348.1	2.900	242.84	412.5	2.064
282.56	466.4	2.901	252.82	504.1	2.065
292.70	623.0	2.902	262.86	610.6	2.066
$z_1 = 0.160$					
223.28	95.7	2.938	272.84	734.4	2.067
233.00	129.7	2.939	282.62	884.2	2.068
242.68	174.3	2.940	$z_1 = 0.574$		
252.82	234.8	2.942	223.63	312.0	2.153
262.80	313.0	2.943	233.01	387.5	2.154
272.75	412.9	2.944	243.08	479.4	2.155
282.57	537.9	2.945	253.03	574.3	2.156
$z_1 = 0.266$					
223.62	147.7	2.569	262.96	686.0	2.157
233.09	190.8	2.570	272.82	813.7	2.158
243.03	246.0	2.571	$z_1 = 0.662$		
252.95	315.1	2.572	223.07	420.2	1.227
262.95	401.7	2.573	232.97	559.0	1.227
272.93	509.9	2.574	242.95	711.4	1.228
282.75	641.4	2.575	252.90	876.2	1.228
292.75	804.6	2.577	262.94	1044.0	1.229
$z_1 = 0.365$					
223.08	197.6	2.253	272.83	1223.1	1.229
232.97	252.9	2.254	282.64	1417.7	1.230
242.99	322.1	2.255	$z_1 = 0.754$		
252.69	399.3	2.256	224.20	460.3	1.747
262.58	492.3	2.257	233.06	576.0	1.747
			243.04	710.6	1.748
			253.04	842.3	1.749
			263.01	980.1	1.750

**VLE Derivation.** The method used to derive VLE data from the isochoric measurements using the Carnahan–Starling–DeSantis

Table 4. Experimental Molar Volumes  $V$  as a Function of Pressure  $P$  and Temperature  $T$  at Composition  $z_1$  in the Superheated Vapor Region for the  $\text{CO}_2$  (1) + R1234yf (2) System

$T$ K	$P$ kPa	$V$ $\text{dm}^3\cdot\text{mol}^{-1}$	$T$ K	$P$ kPa	$V$ $\text{dm}^3\cdot\text{mol}^{-1}$
$z_1 = 0.051$					
302.81	736.5	2.904	302.61	742.4	2.948
303.05	738.0	2.904	307.54	758.8	2.949
312.94	773.7	2.905	313.12	778.4	2.949
322.75	808.1	2.906	323.09	811.8	2.951
333.09	843.3	2.907	333.08	844.9	2.952
343.06	877.3	2.909	343.05	877.5	2.953
353.02	910.7	2.910	352.99	909.5	2.954
362.92	943.3	2.911	362.96	941.6	2.956
372.92	975.7	2.912	372.89	973.3	2.957
$z_1 = 0.160$					
292.47 <sup>a</sup>	673.8 <sup>a</sup>	2.947 <sup>a</sup>	302.88	856.1	2.578
302.61	742.4	2.948	312.82	895.4	2.579
307.54	758.8	2.949	312.82	895.4	2.579
313.12	778.4	2.949	323.10	934.8	2.580
323.09	811.8	2.951	333.08	972.6	2.581
333.08	844.9	2.952	343.04	1010.2	2.582
343.05	877.5	2.953	353.00	1046.2	2.583
352.99	909.5	2.954	362.92	1082.5	2.584
362.96	941.6	2.956	372.89	1119.0	2.586
372.89	973.3	2.957	$z_1 = 0.365$		
$z_1 = 0.266$					
302.88	856.1	2.578	292.85 <sup>a</sup>	906.8 <sup>a</sup>	2.260 <sup>a</sup>
312.82	895.4	2.579	302.96	976.1	2.261
323.10	934.8	2.580	312.92	1020.4	2.262
333.08	972.6	2.581	322.60	1062.1	2.263
343.04	1010.2	2.582	333.07	1106.6	2.264
353.00	1046.2	2.583	343.03	1149.4	2.265
362.92	1082.5	2.584	352.99	1191.4	2.266
372.89	1119.0	2.586	362.92	1232.6	2.267
$z_1 = 0.365$					
272.98	1122.7	1.750	$z_1 = 0.480$		
282.63	1179.9	1.751	292.60	1003.3	2.069
292.67	1237.7	1.752			
302.67	1296.0	1.753			
312.70	1352.4	1.753			
323.10	1407.6	1.754			
333.08	1460.2	1.755			
343.07	1512.6	1.756			
353.02	1564.1	1.756			
362.96	1615.2	1.757			

<sup>a</sup>Not considered in the regression.

equation of state (CSD EoS) was described elsewhere.<sup>7</sup> The CSD EoS was adopted in the following form:

$$\frac{PV}{RT} = \frac{1 + Y + Y^2 - Y^3}{(1 - Y)^3} - \frac{a}{RT(V + b)} \quad (1)$$

where

$$Y = \frac{b}{4V} \quad (2)$$

The method involves deriving the VLE parameters for each data point in the two-phase region using the “flash method” with the CSD EoS. For this method to be applied to isochoric data, we also

**Table 5. Composition at Bubble Point  $x$  (1), Composition at Dew Point  $y$  (1), Bubble-Point Pressure ( $P_B$ ), and Dew-Point Pressure ( $P_D$ ) Derived with the CSD EoS<sup>6</sup> in the Two-Phase Region for the CO<sub>2</sub> (1) + R1234yf (2) System**

$x$ (1)	$y$ (1)	$P_B$		$P_D$		$x$ (1)	$y$ (1)	$P_B$		$P_D$	
		kPa		kPa				kPa		kPa	
$z_1 = 0.051$						0.108	0.500	1331.7			483.5
0.024	0.324	82.4	43.6			0.096	0.430	1677.5			674.6
0.021	0.264	116.4	66.3			$z_1 = 0.480$					
0.018	0.205	169.6	104.2			0.301	0.880	404.1			78.5
0.016	0.159	240.9	157.8			0.269	0.846	534.5			115.9
0.014	0.122	335.5	232.7			0.233	0.794	740.4			183.1
0.012	0.095	453.7	330.0			0.201	0.732	997.6			278.8
0.011	0.075	597.2	452.4			0.175	0.664	1311.0			411.4
0.010	0.059	782.9	615.9			0.154	0.592	1680.8			588.4
$z_1 = 0.160$						0.137	0.523	2101.4			815.3
0.077	0.625	156.7	45.0			$z_1 = 0.574$					
0.066	0.540	225.2	73.7			0.377	0.910	442.0			87.2
0.057	0.457	313.4	115.1			0.328	0.876	622.5			139.9
0.049	0.377	430.7	176.5			0.281	0.828	868.7			222.2
0.042	0.308	574.7	259.4			0.241	0.770	1171.5			337.6
0.037	0.249	750.2	369.5			0.209	0.705	1538.0			496.0
0.033	0.202	958.2	510.6			0.183	0.637	1968.3			706.4
$z_1 = 0.266$						$z_1 = 0.662$					
0.142	0.760	235.2	52.2			0.550	0.949	486.0			104.7
0.123	0.693	331.3	84.2			0.507	0.930	701.6			172.6
0.106	0.615	459.7	133.1			0.459	0.903	980.4			272.7
0.091	0.536	619.8	202.1			0.410	0.869	1327.5			414.2
0.079	0.458	816.8	297.2			0.365	0.825	1754.0			610.9
0.070	0.387	1053.0	424.2			0.326	0.775	2253.5			871.2
0.062	0.324	1326.7	586.6			0.294	0.720	2829.8			1211.1
0.056	0.269	1650.6	798.0			$z_1 = 0.754$					
$z_1 = 0.365$						0.590	0.954	563.7			147.2
0.217	0.838	298.2	58.2			0.529	0.934	784.7			228.8
0.188	0.783	426.2	96.2			0.458	0.903	1101.3			360.2
0.162	0.718	591.5	152.6			0.393	0.862	1500.2			546.7
0.141	0.649	790.0	229.7			0.339	0.811	1987.7			802.6
0.123	0.575	1034.6	337.0			0.590	0.954	563.7			147.2

**Table 6. Coefficients of the CSD EoS<sup>7</sup> for R1234yf**

	$a_0$	$a_1$	$a_2$	$b_0$	$b_1$	$b_2$
carbon dioxide	1324.8179	$-3.8522 \cdot 10^{-3}$	$-8.8413 \cdot 10^{-7}$	0.0680	$-1.0770 \cdot 10^{-4}$	$-2.3529 \cdot 10^{-8}$
R1234yf	3939.9449	$-2.6782 \cdot 10^{-3}$	$-1.5475 \cdot 10^{-6}$	0.1717	$-2.1467 \cdot 10^{-4}$	$-5.0706 \cdot 10^{-8}$

need the volumetric properties of both phases, which were calculated from the CSD EoS.  $T$ ,  $z_i$ , and  $n$  (number of moles charged) were kept constant during the correlation having the isochoric cell volume from the gravimetric calibration, the objective function:

$$Q = \sum_i \left( \frac{dP}{P} \right)^2 \quad (3)$$

was minimized by tuning the binary interaction parameter value,  $K_{12}$ . The average of the value was found to be  $K_{12} = -0.010$ , with a statistical uncertainty of  $\pm 0.005$ . The correlation gives also the parameters of VLE (pressure and composition of both phases) which were considered, obviously, as dependent variables. The values of composition at bubble point, composition at dew point, bubble-point pressures, and dew-point pressures derived with the CSD EoS<sup>6</sup> are reported in Table 5.

For pure compounds, the temperature dependence of parameters  $a$  and  $b$  in the CSD EoS<sup>6</sup> is described by the following

expressions:

$$a = a_0 \cdot \exp(a_1 T + a_2 T^2) \quad (4)$$

$$b = b_0 + b_1 T + b_2 T^2 \quad (5)$$

The  $a_i$  and  $b_i$  coefficients for R1234yf and carbon dioxide are reported in Table 6. Figure 3 shows the scatter diagram of the relative pressure deviations. The pressure deviations were found to be within  $\pm 1\%$  for all series, except few points at lower temperatures measured for series 3. A very different trend of results was obtained comparing the experimental data together with the REFPROP 9.0<sup>8</sup> prediction, which calculations are based on an equation of state explicit in reduced Helmholtz energy.<sup>9</sup>

Here, deviations up to 40% and a generally strong disagreement was evident with experimental data, increasing with the lowering of temperatures, as shown in Figure 4. Since both pure fluids' behavior was well-predicted by the REFPROP 9.0, the revealed discrepancy was probably due to the predictive method

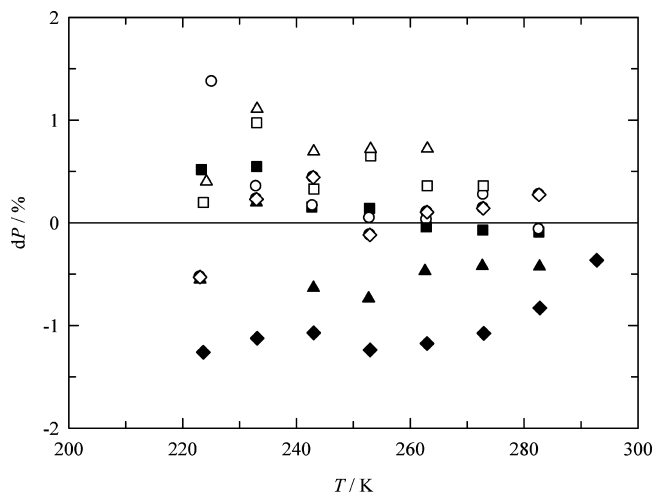


**Figure 3.** Pressure deviations between experimental values and those calculated with the CSD EoS<sup>7</sup> for the CO<sub>2</sub> (1) + R1234yf (2) system in the two-phase region. Symbols are denoted as in Figure 2.

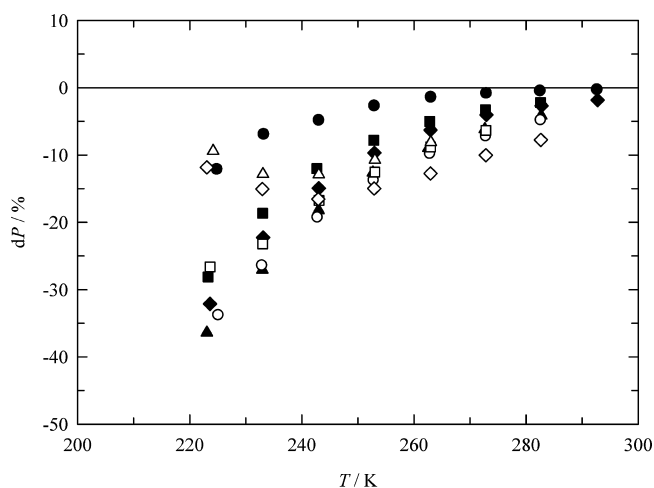


**Figure 4.** Pressure deviations between experimental values and those calculated with the REFPROP 9.0<sup>8</sup> for the CO<sub>2</sub> (1) + R1234yf (2) system in the two-phase region. Symbols are denoted as in Figure 2.

applied in the estimation of binary interaction parameters, since no experimental mixture data were available for this system.

The VLE behavior of the system was also calculated at three fixed temperatures, (233.15, 253.15, and 273.15) K, with the CSD EoS<sup>7</sup> adopting the found binary interaction parameter  $K_{12} = -0.010$ . The system showed small deviations from Raoult's law for all of the temperatures, as shown in Figure 5.

**PVTx.** Data on the superheated vapor region for the binary systems considered were also compared with the CSD EoS<sup>6</sup> and REFPROP 9.0<sup>8</sup> prediction. In this case, the averaged value of  $K_{12} = -0.010$  obtained with the flash method in the two-phase region data was used for the CSD EOS calculations. Not considering the points in the proximity of the change of phase that showed much higher deviations (these points were denoted in Table 4 with an asterisk), an AAD ( $dP\%$ ) = 0.24 % was obtained. Again, deviations within  $\pm 1\%$  for all series were obtained with the CSD EoS, except few points at lower temperatures. Slightly higher deviations were achieved comparing the experimental findings with the REFPROP 9.0 prediction, obtaining an AAD ( $dP\%$ ) = 0.64 %. Results are summarized in Figures 6 and 7.

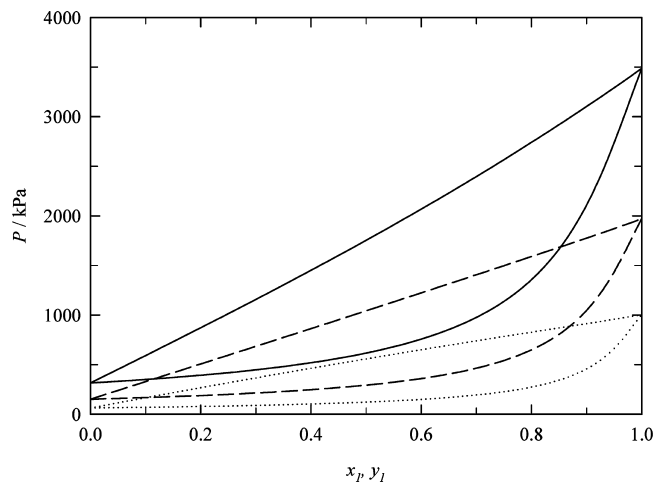


**Figure 5.** VLE representation from the correlation with the CSD EoS<sup>6</sup> for the CO<sub>2</sub> (1) + R1234yf (2) system at three temperatures: dotted lines,  $T = 233.15$  K; dashed lines,  $T = 253.15$  K; solid lines,  $T = 273.15$  K.

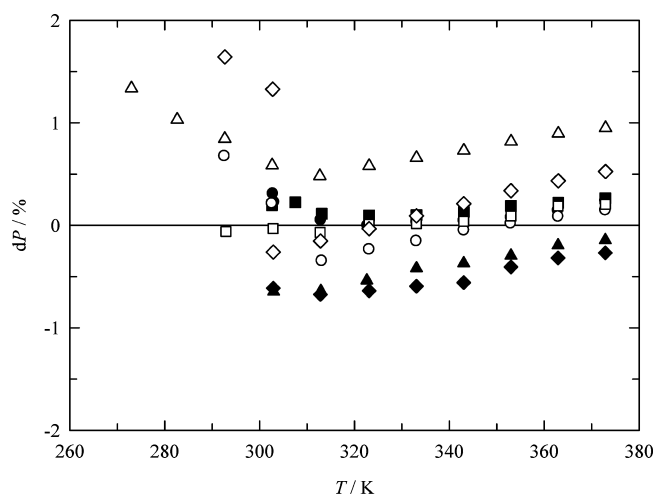


**Figure 6.** Pressure deviations between experimental values and those calculated with the CSD EoS<sup>7</sup> for the CO<sub>2</sub> (1) + R1234yf (2) system in the superheated vapor region. Symbols are denoted as in Figure 2.

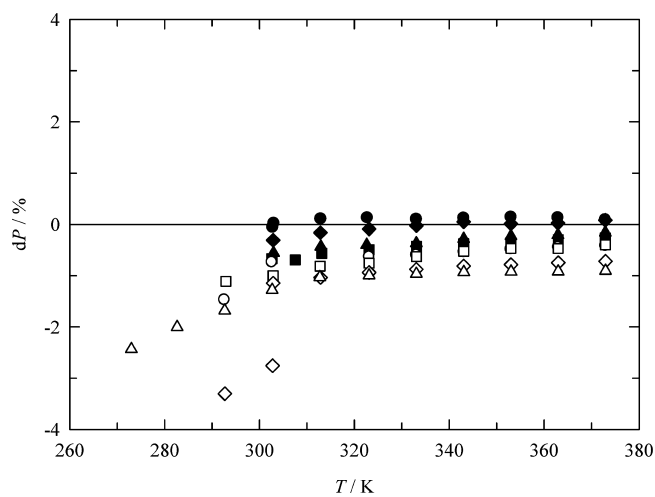


**Figure 7.** Pressure deviations between experimental values and those calculated with the REFPROP 9.0<sup>8</sup> for the CO<sub>2</sub> (1) + R1234yf (2) system in the superheated vapor region. Symbols are denoted as in Figure 2.

## ■ CONCLUSIONS

An isochoric apparatus has been used to obtain  $PVT_x$  measurements on  $\text{CO}_2 + \text{R1234yf}$ . The binary interaction parameters were derived from experimental data in the two-phase region, applying the flash method and the CSD EoS. The  $PVT_x$  data at superheating region were compared by the CSD EoS and by REFPROP 9.0 prediction.

## ■ AUTHOR INFORMATION

### Corresponding Author

\*E-mail: g.dinicola@univpm.it.

## ■ REFERENCES

- (1) Di Nicola, G.; Polonara, F.; Santori, G. Saturated Pressure Measurements of 2,3,3,3-Tetrafluoroprop-1-ene (HFO-1234yf). *J. Chem. Eng. Data* **2010**, *55*, 201–204.
- (2) Di Nicola, C.; Di Nicola, G.; Pacetti, M.; Polonara, F.; Santori, G.  $P$ – $V$ – $T$  Behavior of 2,3,3,3-Tetrafluoroprop-1-ene (HFO-1234yf) in the Vapor Phase from (243 to 373) K. *J. Chem. Eng. Data* **2010**, *55*, 3302–3306.
- (3) Di Nicola, G.; Giuliani, G.; Polonara, F.; Stryjek, R. Blends of carbon dioxide and HFCs as working fluids for the low-temperature circuit in cascade refrigerating systems. *Int. J. Refrig.* **2005**, *28*, 130–140.
- (4) Di Nicola, G.; Polonara, F.; Stryjek, R.; Arteconi, A. Performance of cascade cycles working with blends of  $\text{CO}_2 + \text{natural refrigerants}$ . *Int. J. Refrig.* **2011**, *34*, 1436–1445.
- (5) Di Nicola, G.; Polonara, F.; Ricci, R.; Stryjek, R.  $PVT_x$  Measurements for the R116 +  $\text{CO}_2$  and R41 +  $\text{CO}_2$  Systems. New Isochoric Apparatus. *J. Chem. Eng. Data* **2005**, *50*, 312–318.
- (6) Giuliani, G.; Kumar, S.; Polonara, F. A constant volume apparatus for vapour pressure and gas phase  $P$ – $v$ – $T$  measurements: validation with data for R22 and R134a. *Fluid Phase Equilib.* **1995**, *109*, 265–279.
- (7) De Santis, R.; Gironi, F.; Marrelli, L. Vapor-Liquid Equilibrium from a Hard-Sphere Equation of State. *Ind. Eng. Chem. Fundam.* **1976**, *15*, 183–189.
- (8) Lemmon, E. W.; Huber, M. L.; McLinden, M. O. *NIST Standard Reference Database 23: Reference Fluid Thermodynamic and Transport Properties-REFPROP*, Version 9.0; National Institute of Standards and Technology, Standard Reference Data Program: Gaithersburg, MD, 2010.
- (9) Lemmon, E. W.; Tillner-Roth, R. A Helmholtz energy equation of state for calculating the thermodynamic properties of fluid mixtures. *Fluid Phase Equilib.* **1999**, *165*, 1–21.